Modelling exposure to aerosols from showers

Implications for microbial risk assessment

Tang, Lizhan; Eichelberg, Antonia; Böni, Franziska; Hamilton, Kerry A.; Sylvestre, Émile; Hammes, Frederik; Julian, Timothy R

DOI
10.1016/j.buildenv.2025.112825

Publication date
2025

Document Version
Final published version

Published in
Building and Environment

Citation (APA)
Tang, L., Eichelberg, A., Böni, F., Hamilton, K. A., Sylvestre, É., Hammes, F., & Julian, T. R. (2025). Modelling exposure to aerosols from showers: Implications for microbial risk assessment. *Building and Environment*, *275*, Article 112825. https://doi.org/10.1016/j.buildenv.2025.112825

Building and Environment 275 (2025) 112825

Contents lists available at ScienceDirect

Building and Environment

journal homepage: www.elsevier.com/locate/buildenv

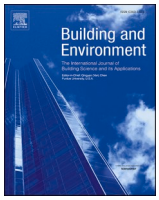

Modelling exposure to aerosols from showers: Implications for microbial risk assessment

Lizhan Tang [a,b], Antonia Eichelberg [a], Franziska Böni [a], Kerry A. Hamilton [c,d], Émile Sylvestre [a,g], Frederik Hammes [a], Timothy R Julian [a,e,f,*]

[a] Eawag, Swiss Federal Institute of Aquatic Science and Technology, Dübendorf 8600, Switzerland
[b] Department of Environmental Systems Sciences, ETH Zürich, Zürich 8092, Switzerland
[c] School of Sustainable Engineering and the Built Environment, Arizona State University, Tempe, Arizona, USA
[d] Biodesign Institute Center for Environmental Health Engineering, Arizona State University, Tempe, Arizona, USA
[e] Swiss Tropical and Public Health Institute, Allschwil 4123, Switzerland
[f] University of Basel, Basel 4055, Switzerland
[g] Sanitary Engineering, Delft University of Technology, Delft, The Netherlands

ARTICLE INFO

Keywords:
Aerosols
Exposure
Showers
Water
Pathogens
Mathematical modeling

ABSTRACT

Inhalation of aerosols produced during showering exposes people to chemical and microbial contaminants present in the water. To improve quantitative estimates of exposure and to inform the efficacy of potential interventions to reduce exposures, the number and size distributions of aerosols generated during showering events were monitored and a mass balance model of the generated aerosols was developed. The aerosol generation rates were calculated through calibrating the model with the measured aerosol data. Specifically, aerosol count concentrations and size distributions were measured with an aerodynamic particle sizer over the duration of mock showering events under various conditions, including different water temperatures and different showerhead types (conventional and rain showers). The empirical data were then used to fit a mass balance model to obtain aerosol generation rates and decay rates for each aerosol size class through least square fitting. An initial high peak concentration of aerosols was observed under hot water conditions relative to cold water conditions which resulted in a rapid increase in aerosol exposure during the first 1–2 min of showering. This suggests that people showering in hot water conditions will have a potentially increased exposure during the first 1–2 min. The model-fitted values suggest large inter-experiment variation in estimated aerosol generation and decay rates, even among triplicates of the same showering conditions. Current exposure assessment approaches assume constant aerosol concentrations during showers which might lead to miscalculated cumulative risk for microbial hazards because of their uneven distribution in building plumbing systems and biofilm detachment process during flushing. Thus, considering aerosol dynamics is beneficial during shower exposure assessments to inform risk management interventions. The data set and associated modeling results provided can support this, as they can be readily integrated into microbial risk assessments for waterborne pathogens such as *Legionella* spp., nontuberculous *Mycobacteria* (NTM) and *Pseudomonas aeruginosa*.

1. Introduction

Waterborne pathogens in drinking water systems such as *Legionella* spp., *Mycobacterium* spp. and *Pseudomonas aeruginosa* increase risks for respiratory diseases during daily activities, such as showering and toilet flushing [14,24]. Inhalation of contaminated aerosols is the major route of exposure, with showers perceived to be of particular concern due to the generation of, and resultant exposure to, high concentrations of inhalable aerosols [19,25,44]. Understanding fate and transport of aerosols in showers can provide insights into exposure pathways leading to respiratory diseases and contribute to the design of effective interventions.

Estimates of aerosol concentrations, fate, and transport in showers are driven by data collected empirically. Parameters related to aerosol

* Corresponding author at: Department of Environmental Microbiology, Eawag, Swiss Federal Institute of Aquatic Science and Technology, Dübendorf 8600, Switzerland.
E-mail address: tim.julian@eawag.ch (T.R. Julian).

https://doi.org/10.1016/j.buildenv.2025.112825
Received 1 November 2024; Received in revised form 3 March 2025; Accepted 5 March 2025
Available online 6 March 2025

concentrations were usually identified as one of the most sensitive parameters for risk assessment [49]. Empirical studies have quantified shower aerosol generation rates and identified factors that influence the aerosol concentration and distribution profile such as water flow rate, water temperature, water pressure, humidity, showerhead characteristics, and ventilation conditions [12,18,35,38,52,56]. Some studies, primarily focused on chemical exposure assessment, collected data on aerosols equal to or smaller than 2.5 μm, a size class particularly relevant due to its deposition in the alveoli and bronchi [52,55]. For aerosols larger than 2.5 μm, many current studies applied general aerosol generation rates or partitioning coefficients (ratio of pathogen in air relative to water) for the respirable fraction [12,18,35,56]. Aerosols ranging between 1 and 10 μm are normally large enough to encapsulate microorganisms and small enough to deposit at alveoli. Submicron aerosols may also contain cellular fragments but these fragments were not considered as viable cells and therefore less likely to cause infections [2]. Submicron aerosols may also contain viruses, as demonstrated in wastewater treatment plants and public fountains (Deere & Ryan, 2022; Heida et al., 2024; Pasalari et al., 2022). For this study which focuses on building plumbing systems serving treated water, bacterial pathogens capable of growing in the system after treatment were the primary focus [49]. Aerosols larger than 5 μm are significantly less likely to deposit at alveoli compared to smaller aerosols according to the International commission on radiological protection (ICRP) lung deposition model [3,54]. However, bacteria such as *Legionella* spp. partitioning into aerosols larger than 5 μm could account for 48% of total airborne bacteria [2]. Therefore, size-resolved generation rates for aerosols within the range of 1–10 μm are needed for reliable microbial risk assessments.

Microbial risk assessments rely on aerosol concentration modeling approaches including volumetric estimation or partitioning coefficient approaches to model exposure to respiratory pathogens for shower scenarios [24,25,42]. Most studies applying these approaches typically measure either aerosols or microorganisms as data input [18,27,55]. Comparatively, few studies investigate both aerosol size distribution and microorganisms in air using impactor cultures for shower-like systems [2,3]. These approaches typically assume constant aerosol concentration over the entire shower duration. A consequence of constant aerosol concentration estimation is the potential to overestimate or underestimate risk, because assumed constant aerosol concentration corresponds to steady state, while aerosol concentration at the increase state (period when aerosol concentration is continuously increasing) is usually ignored. An alternative to volumetric estimation and partitioning coefficient approaches is mass balance model approach, which can incorporate multiple aerosol transport process such as deposition and ventilation following the conservation of mass principle, and therefore be more generalizable. Previous studies focusing on chemical exposure assessment have shown that one compartment models can properly describe dynamic changes of aerosol concentrations [12,55]. Through fitting the mass balance model to experimental measured aerosol data, aerosol generation rates ranging from 44 to 5682 μg/min were obtained depending on different aerosol size classes and showerhead characteristics [12,52,55]. However, constant aerosol generation rates were assumed by these studies and therefore the dynamic change of aerosol concentrations especially for hot showers was not addressed [52,55]. The initial high concentrations of aerosols were ignored by these studies which could be influential on the waterborne pathogen risk assessments considering they were mainly present in the first liter water during flushing due to biofilm detachment [45].

In this study, empirical data collection and modeling of aerosols in showers were advanced. Specifically, (1) the temporal variation of aerosol concentration and size distribution of aerosols under selected conditions with shower experiments were investigated, 2) size-resolved parameters for aerosol generation rates that can be directly used in exposure and risk assessment models were estimated, and (3) a mass balance model that describes temporal variations of aerosol concentrations and corresponding exposures for people showering was developed.

2. Methods

2.1. Experimental overview

Empirical measurements of aerosol concentration and size distribution were collected in the bathroom of a fitness center in Dübendorf, Switzerland (Figure S1). The shower stall had a dimension of 0.9 m (length) × 1.2 m (width) × 2.3 m (height). The shower stall was closed with a glass door, and air exchange was measured for each experiment and was influenced by a ventilation system installed at the top of the shower stall. A conventional showerhead and a rain showerhead (Arwa, Switzerland), both made of stainless steel, were installed in the shower stall. Both types of showerheads were operated at a water pressure of 3 kPa, with a nozzle diameter of 1 mm. The conventional showerhead contained 65 nozzles, whereas the rain showerhead had 210 nozzles. The rain showerhead was installed on the ceiling at a height of 2.3 m above the ground. To ensure aerosols were emitted at the same position, the conventional showerhead was fixed at the same position of the rain showerhead. A mannequin with a height of 1.75 m was positioned right below the rain and conventional showerhead to simulate the presence of a person during the shower and to account for secondary formation of aerosols due to water splashing onto human skin. The mannequin had a shoulder width of 0.4 m, a chest circumference of 0.81 m, a waist circumference of 0.61 m and a hip circumference of 0.86 m. The mannequin's surface was smooth and made of hydrophobic polyethylene plastic.

Two water temperatures (moderately cold at 25–28 °C and moderately hot at 39–41 °C) and two showerhead types (conventional and rain) were tested to assess aerosol concentration and size distribution. The water flow rates were 10 L/min for the rain showerhead and 8 L/min for the conventional showerhead when the fixture handle is fully open by the user. Water flow rates were kept constant throughout the duration of the shower. The aerosol size distributions and concentrations were measured with an aerodynamic particle sizer (APS; 3321, TSI Inc, U.S.A.). Aerosols were sampled using tubes connected to the inlet port of APS with a total flow rate of 5 L/min (1 L/min for aerosol sampling and 4 L/min for sheath air). Considering longer tubing can cause particle loss due to inertial impaction, diffusional deposition, gravity deposition and thermophoretic deposition, a location 1 m above ground within the shower stall was chosen for aerosol sampling and further exposure modeling. The APS was placed on a table and connected with a 0.1 m tube. In addition, two other locations (1.8 m above ground and 2.2 m above ground) were sampled with longer tubes (1.2 m and 1.5 m in length) to investigate the spatial variations of aerosol size distributions. The outputs of APS are size distribution normalized by aerosol size and aerosol count for each aerosol size class, which included 32 channels within the size range of 0.5 to 20 μm. Aerosol data collection was performed using Aerosol Instrument Manager software (AIM 10.3, TSI Inc, U.S.A.), with measurements recorded every 20 s. The data collected by AIM software were raw counts of aerosols in different size bins at a sampling flow rate of 1 L/min (i.e., 0.33 L of air was sampled for each 20 second interval). The number concentrations were obtained by dividing the raw counts by sampled air volume (0.33 L). These number concentrations were then converted to mass concentrations, considering that the equipment measured aerodynamic diameter under the assumption of a particle density of 1 g/cm^3 and a spherical particle shape.

Measurements were collected for 5 min prior to the shower being turned on to measure the background aerosol concentration. Then, the shower was turned on for 10 min to mimic a typical shower length [30,46]. Following this, the shower was turned off but aerosols were continuously measured for an additional 5 min to allow measurements of the decay of aerosol concentrations back to the background. To measure the ventilation rate, carbon dioxide (CO_2) was used as a tracer gas [8]. CO_2 was injected from a compressed gas cylinder into the shower stall until an initial concentration of 3000–4000 ppm was

reached. This concentration was well below the American Conference of Governmental and Industrial Hygienists' recommended 8-hour Time Weighted Average Threshold Limit Value [6] while also being sufficiently above background to enable estimation of ventilation rate. Before CO_2 concentration measurements were taken, a fan was used to ensure thorough mixing of air. The decay of CO_2 concentration was then recorded using Vitales 501 CO_2 monitor (Vitales 501, Vitales, Switzerland). Through fitting an exponential decay model to the measured concentrations over time, the ventilation rate was estimated [55]. The CO_2 monitor also recorded relative humidity and temperature every 20 s.

2.2. Aerosol concentration modeling

2.2.1. Mass balance model

To estimate exposure for a person enclosed within a shower stall, a mass balance model was used [54]. Assuming a closed system following the principle of mass conservation and accounting for the generation rate from the shower and decay from ventilation, deposition, and other processes, the mass concentration of aerosol was predicted as follows:

$$V_m \frac{dc_i}{dt} = -\left(Q + \sum v_{i,j} S_j + \lambda_i V_m\right) \cdot c_i + G_i \quad (1)$$

where V_m is the volume of the shower stall (m^3), c_i is the mass concentration of aerosol of size i ($\mu g/m^3$), t is the exposure duration (min), Q is the ventilation rate or air flow rate (m^3/min); S_j is the area of vertical, upward-facing, and downward-facing surface j within the shower stall (m^2); $v_{i,j}$ is the deposition velocity of aerosol of size i for the surface j (m/min) which is predominantly driven by gravity forces for micro-sized aerosols; λ_i is the aerosol residual decay rate caused by other removal process excluding deposition and ventilation rate for aerosol of size i (1/min) (e.g., evaporation, inertial impaction and interception); G is the generation rate of aerosol of size i (μg/min).

The deposition velocities were calculated following the method proposed by Lai and Nazaroff [32].

2.2.2. Model calibration

The mass balance model was fitted to measured aerosol concentrations for each aerosol size class using the least squares method [34]. Aerosol generation rate and aerosol decay rate were treated as unknown parameters during the model fitting. The fitting process was conducted using the differential equations solver Berkeley Madonna (version 9.1.19, University of California at Berkeley, U. S. A.) with the Rosenbrock algorithm for stiff differential equations.

2.2.3. Estimating exposure to the respirable fraction of aerosols

The potential inhalation dose of aerosols for a single shower event was calculated using the following equation:

$$D = \int_{t_1}^{t_2} \sum_{i=1} C_{aer,i} D_i B dt \quad (2)$$

where D is the inhalation dose of aerosols (g), $C_{aer,i}$ is the mass concentration of aerosols of size i (g/m^3), B is the inhalation rate for average of male and female (m^3/min) [17,47], and D_i is the deposition fraction of an aerosol of size i at human alveoli, t_1 is the time when people enter shower stall and t_2 is the time when people leave shower stall (min). The detailed calculation of deposition fraction D_i was provided in supporting information.

Exposure modeling, including estimating uncertainty and variability of model output, was conducted using Monte Carlo simulations in R (v4.4.1, Bell Laboratories Inc, U. S. A.) and RStudio (v2024.04.2 + 764, Posit PBC, U. S. A.) (www.rproject.org), based on 10,000 iterations. Distributions of all relevant aerosol and exposure parameter values were provided in Table S1.

2.2.4. Statistical analysis

All statistics were conducted using R (v4.4.1, Bell Laboratories Inc, U. S. A.) and RStudio (v2024.04.2 + 764, Posit PBC, U. S. A.). A t-test was used to compare geometric mean diameters of aerosols produced and aerosol generation rates at different selected conditions (i.e. hot shower vs cold shower, conventional showerhead vs rain showerhead).

3. Results

3.1. Aerosol size distribution

Aerosol size distributions were generally consistent throughout the shower. No significant change was observed regarding the geometric mean diameter of aerosols generated from the start of the shower (1 min after turning on shower) and end of the shower (1 min before turning off shower) (Table 1) ($p = 0.6$, t-test), but differences were observed when comparing the geometric mean diameters between the cold-water scenarios and hot water scenarios ($p = 6.7 \times 10^{-9}$, t-test). Geometric mean diameters for aerosols generated using the conventional showerhead at the 1st and 10th minutes were similar to the geometric mean diameters generated using the rain showerhead ($p = 0.7$, t-test). For cold water scenarios, the majority of aerosols generated by the two types of showerheads were smaller than 5 μm and smaller aerosols accounted for a higher fraction of total number concentrations (Fig. 1). Comparatively, aerosols generated by hot water showers were larger than aerosols generated by cold water showers and were characterized by a bimodal distribution (Fig. 1 and Table 1).

3.2. Concentration of aerosols over time

The concentration profile of aerosols generated during and after the shower can be divided into 3 phases: 1) increase state (1–2 min after the shower was turned on), 2) steady state (1–2 min after shower is turned on), and 3) decay state (after the shower was turned off). For cold water scenarios, the concentration of aerosols increased exponentially during the increase state (Figs. 2,3). In many scenarios, a plateau in aerosol concentrations indicating steady state was reached. In other scenarios, the aerosol concentrations continuously increased until the end of the shower and a steady state concentration was not reached (Figure S2, Figure S3). The specific scenario depended on the air exchange rate within the shower, with higher air exchange rates reaching steady state faster than lower air exchange rates, as expected from the mass balance model.

For hot water scenarios, an almost instantaneous increase of aerosol concentration after the shower was turned on was observed in all experiments (Fig. 3). After approximately 1 min, a peak concentration was reached and then aerosol concentrations decreased exponentially until reaching a steady state (Fig. 3). Notably, the peak concentration was sometimes 2–3 times higher than the steady state concentration (Fig. 3). After the shower was turned on, both air temperature and relative humidity (RH) also gradually increased (Figure S6. For hot water scenarios, the highest air temperature at steady state was around 30 °C and the relative humidity gradually increased to 95% (Figure S6). For cold water scenarios, the rapid increase in aerosol concentrations was not observed, and the air temperature eventually reached approximately 27 °C which was close to the cold water temperature. The background RH, ranging from 50% to 80%, gradually increased to 85% under cold water conditions and 95% under hot water conditions (Figure S6).

3.3. Aerosol generation rates and decay rates

A mass balance model was fit to measured aerosol concentrations to get size-resolved aerosol generation rates and decay rates (Fig. 2, Fig. 3). The model fitting was conducted on each of the three phases separately to allow estimation of distinct aerosol generation rates and decay rates. For cold water scenarios, a constant aerosol generation rate for the

Table 1
Summary of aerosol size distribution under selected conditions. Note: The beginning of the shower refers to 1 min after turning on shower and the end of the shower refers to 1 min before turning off shower.

Experiment run	Water temperature (°C)	Showerhead type	Water flow rate (L/min)	Geometric mean diameter of generated aerosols (μm)			
				Beginning of the shower	Average ± standard deviation	End of the shower	Average ± standard deviation
1	25.9	Rain	10	0.95	0.96 ± 0.01	1.07	1.00 ± 0.06
2	25.8	Rain	10	0.96		0.96	
3	27.3	Rain	10	0.97		0.99	
4	29.3	Conventional	8	0.85	0.98 ± 0.14	0.97	1.03 ± 0.06
5	27.8	Conventional	8	1.12		1.03	
6	26.6	Conventional	8	0.97		1.09	
7	39.7	Rain	10	5.03	5.18 ± 0.13	6.34	6.19 ± 0.78
8	41.9	Rain	10	5.29		6.89	
9	41	Rain	10	5.22		5.35	
10	40	Conventional	8	4.1	4.52 ± 0.86	5.18	5.32 ± 1.25
11	40.5	Conventional	8	5.51		6.63	
12	39.5	Conventional	8	3.96		4.15	

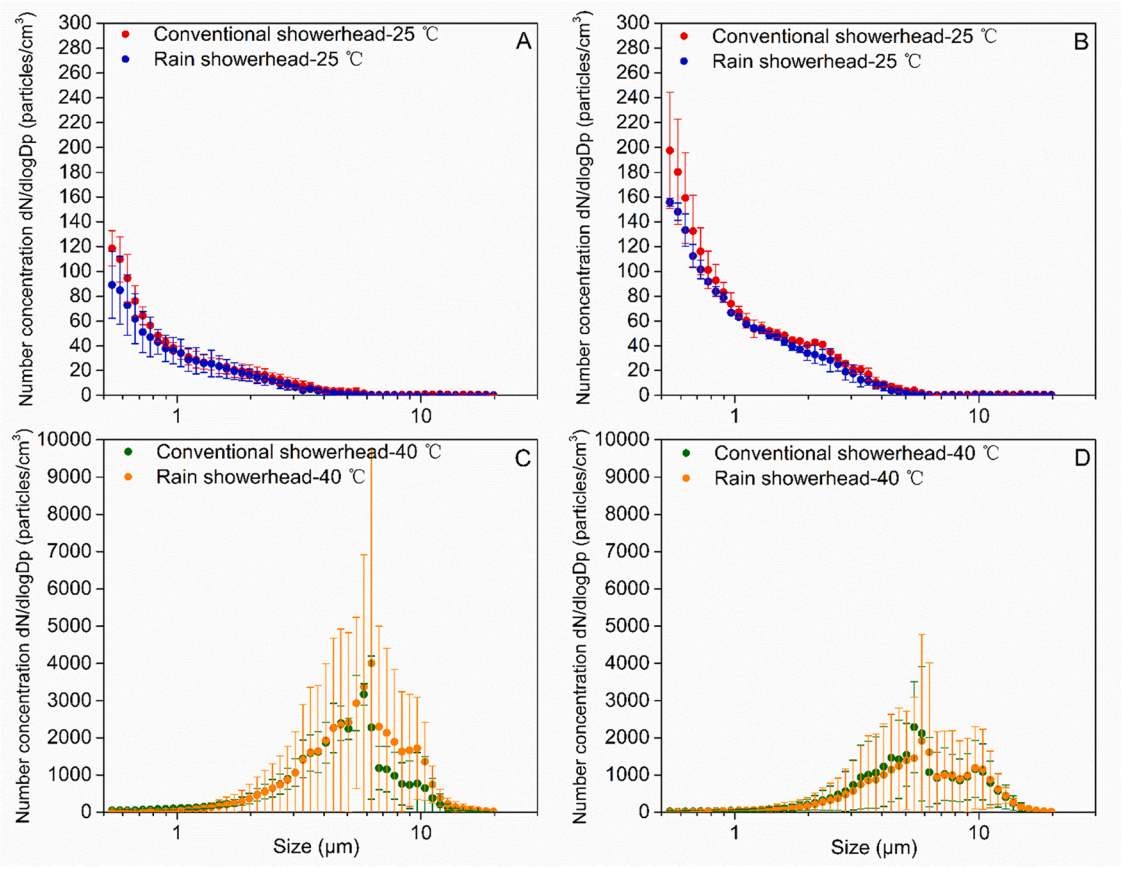

Fig. 1. Size distribution as total number concentration at the beginning of cold showers (A), at the end of cold showers (B), at the beginning of hot showers (C) and at the end of hot showers (D).
Note: The beginning of the shower refers to 1 min after turning on showers and the end refers to 1 min before turning off the showers. The error bars represent standard deviation of measurement results. The sizes of particles were presented as aerodynamic diameters. The beginning refers to 1 min after turning on the shower and the end refers to 1 min before turning off the shower.

increase and steady state phases (i.e. a single generation rate for the entire shower) was assumed considering that the water flow rates were kept constant, and the showerheads and mannequin were fixed throughout the duration of the showers. For hot water scenarios, because of the empirically observed rapid initial increase of aerosol concentration, the increase and steady states were modeled as two distinct aerosol generation rates (i.e. a higher generation rate for the first 1–2 min and a lower generation rate after the first 1–2 min). For both cold and hot water scenarios, two distinct aerosol decay rates were applied: one rate for when the shower was turned on and a separate decay rate for when the shower was turned off, considering environmental conditions such as ambient temperature and relative humidity can be different when the shower is on or off.

Total aerosol generation rates were not significantly different between two types of showerheads ($p = 0.5$, t-test). Total aerosol generation rates for hot water scenarios were up to three orders of magnitude higher than those for cold water scenarios (Table 2, Table 3) ($p = 0.04$, t-test). In hot scenarios, aerosols ranging from 5 to 6 μm have the highest

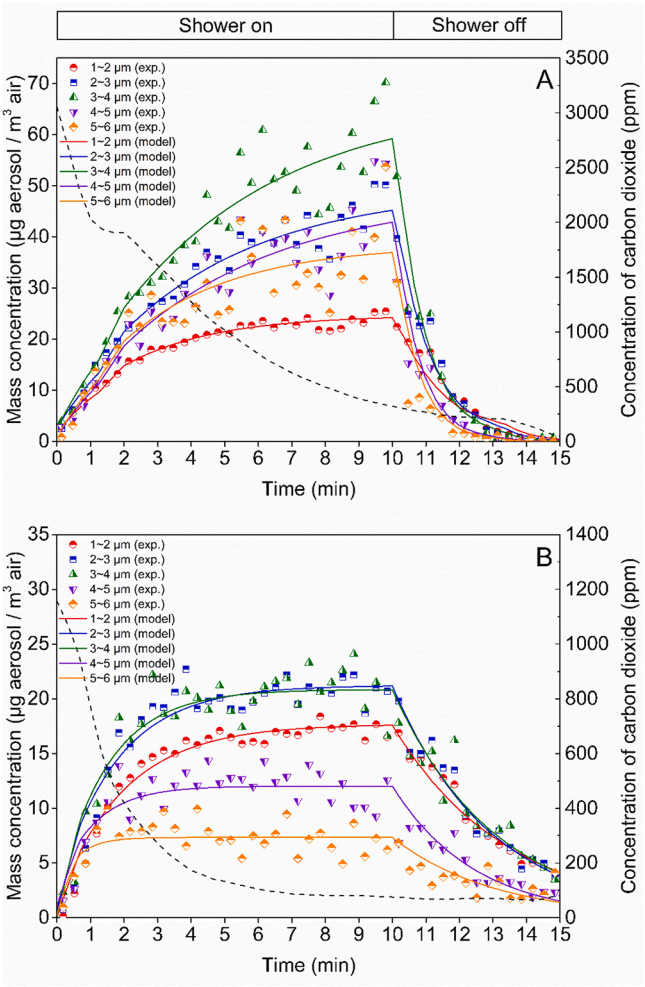

Fig. 2. Concentration of aerosols ranging between 1 and 6 μm at cold water temperature generated by conventional showerhead (A) and rain showerhead (B).

Note: The data are for experiment runs 3 and 6 described in Table 1. The term exp refers to the experimentally collected data, and model refers to the model fit values. The black dashed lines represent measured CO_2 concentrations subtracting background CO_2 concentrations. The sizes of particles were presented as aerodynamic diameters.

generation rates both by count and mass. Notably, in hot water conditions, the aerosol generation rates during the increase state were 2–4 times higher than those during the steady state.

In the one compartment model, an additional parameter fit to the model was a parameter to estimate the residual aerosol decay rate (λ) to account for aerosol removal processes that occur in addition to the ventilation and deposition removal processes. This rate is intended to represent combinations of other potential removal processes, such as evaporation, coagulation, impaction, interception, and thermophoresis. Residual aerosol decay rates close to 0 would indicate the aerosol removal processes beyond ventilation and deposition are negligible. Based on fitted values, the residual aerosol decay rates under cold water conditions (Table 2) were much closer to 0 than those under hot water conditions (Table 3). Specifically, it was found that fitted residual aerosol decay rates for the rain showerhead under hot water conditions were both higher and more variable than the other scenarios. Higher residual aerosol decay rates were observed during the decay phase (e.g., when the shower was turned off) compared to the increase and steady state phases (e.g., when the shower was turned on).

Aerosol generation rates were used to estimate aerosol exposures through inhalation under all tested conditions (Fig. 4). The estimated mean cumulative doses for inhalation of aerosols under hot water conditions, calculated based on the area under the curve, was 885.8 μg for conventional showerhead and 557.6 μg for rain showerhead, which was two orders of magnitude higher than cold water estimates of 5.0 μg for conventional showerhead and 1.5 μg for rain showerhead. For hot water scenarios, the slope of increase for the initial 2 min was higher than the remaining period due to the initial peak concentration of aerosols during the increase state (Fig. 4). Comparatively, the slope of increase for cold water scenarios was much lower due to the low aerosol generation rates. After the shower was turned off, a continued exposure increase was observed for cold water scenarios while the exposure for hot water scenarios reached a plateau. This is because, under hot water scenarios, the aerosol concentration typically decreased dramatically, reaching almost undetectable once the showerhead is off, whereas the aerosol concentration decreased more slowly under cold water scenarios.

4. Discussion

4.1. Aerosol generation rates were more influenced by water temperature than by showerhead type

Showerhead types had little influence on aerosol concentration and size distribution, whereas temperature had a larger effect. The observation reported here of a minimal impact of showerheads may be due to the study design, which looked at a single, constant flow rate for each shower type, and the flow rates for the two showerhead types were similar: 8 and 10 L/min. Studies have shown that showerhead characteristics such as water flow rate, water pressure, number of nozzles and spray angle can influence aerosol emission to different extents [35,55]. However, the difference in aerosol generation rates caused by showerhead characteristics may be low, typically reported as within 1 $\log_{10}$ [18,41,52]. Comparatively, water temperature differences can result in 2–3 $\log_{10}$ differences in aerosol generations rates [55]. This finding is consistent with previously reported results on the importance of temperature in aerosol generation rates, and highlights that risk mitigation strategies focused on reducing water temperatures may see greater reductions in aerosol exposures than strategies focused on changing showerhead characteristics. However, it should be noted that this study only focused on aerosol exposures without considering impact of testing conditions on microorganisms. Water temperature as well as water flow rate (e.g., water-saving showerheads) could also impact microbial densities and viability in aerosols which could also influence the final risk outcomes [11,37,41]

The observed higher aerosol concentrations under hot water scenarios, particularly during the steady state phase, may be due to increased humidity (Figure S6). Water at higher temperatures evaporates faster and therefore leads to higher relative humidity (i.e., higher concentrations of water vapor) compared to cold water [1,50]. Due to the temperature difference between hot water and ambient air, the heat transfer from hot water to ambient air leads to an increase in air temperature. The heated air carrying concentrated hot water vapor will move upward and expand due to the thermal plume effect [55]. Subsequently, rapid condensation can happen once the hot humidified air reaches relatively colder shower stall walls because of the high relative humidity and the low temperature of the shower stall walls [12,15,16]. For micro-sized droplets, the vapor pressure at the droplet surface needed to maintain a specific size (i.e., no condensation and evaporation) can be considered equal to the saturation vapor pressure considering micro-sized droplets are less impacted by the Kelvin effect than submicron droplets [33].

4.2. Aerosol decay rates vary at different stages and different water temperature conditions

In the one compartment model presented here, the non-zero values of fitted aerosol decay rates (λ) suggests that there are processes

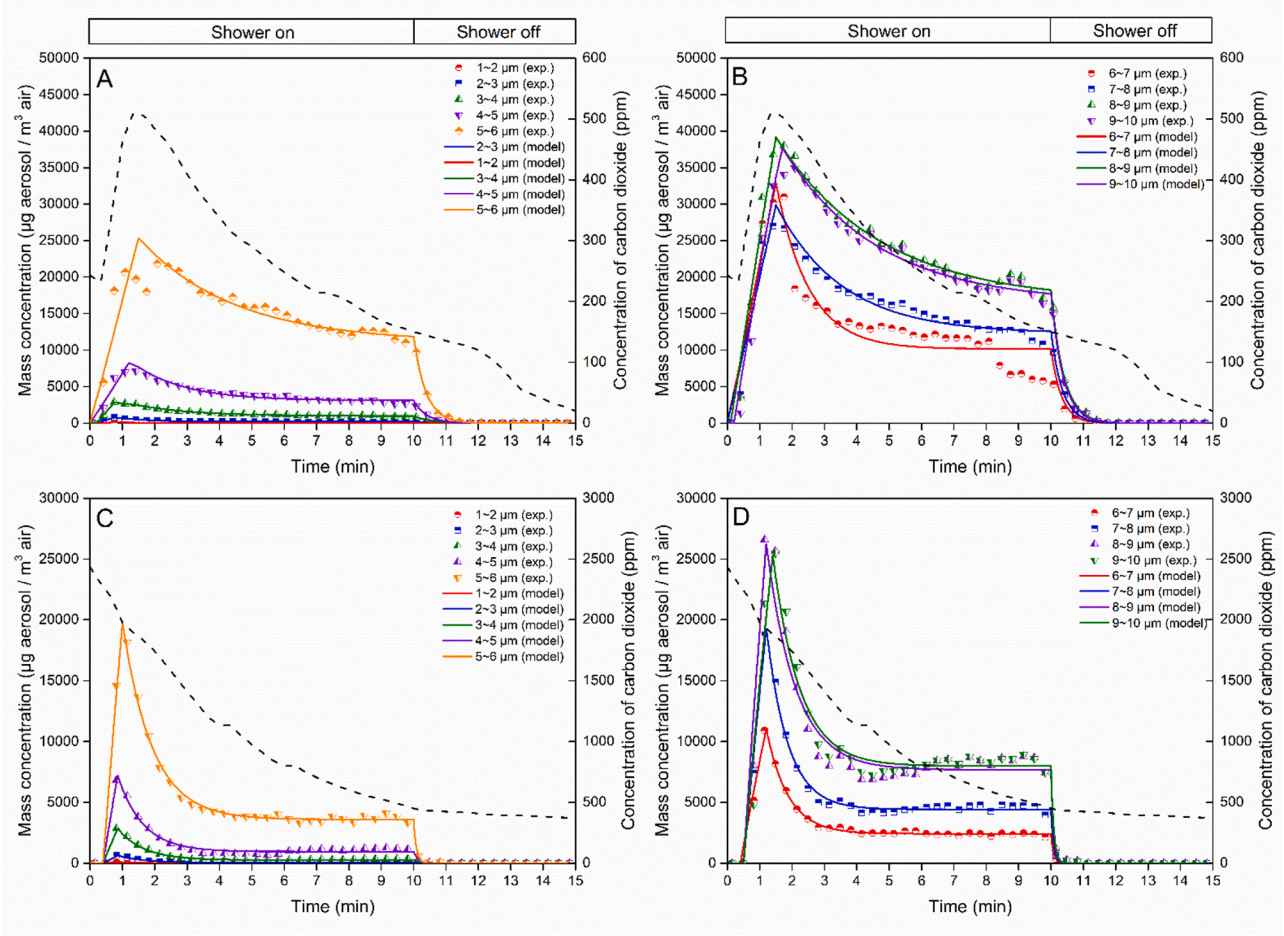

Fig. 3. Concentration of aerosols ranging between 1 and 6 μm at hot water temperature generated by conventional showerhead (A) and rain showerhead (C) as well as aerosols ranging between 6 and 10 μm at hot water temperature generated by conventional showerhead (B) and rain showerhead (D).
Note: The data are for experiment run 8 and 11 in Table 1. The term exp refers to the experimentally collected data, and model refers to the model fit values. The black dashed lines represent measured CO_2 concentrations subtracting background CO_2 concentrations. The sizes of particles were presented as aerodynamic diameters.

Table 2
Model-fitted aerosol generation rates and decay rates under cold water conditions. Note: Aerosol decay rate excludes ventilation rate and deposition rate. SD refers to Standard Deviation, Rain refers to the rain showerhead type, and Conventional refers to the conventional showerhead type.

Showerhead type	Flow rate (L/min)	Size range (μm)	Aerosol generation rate (μg/min)		Decay rate (1/min)				Water temperature (℃)	
					Increase state and steady state		Decay stage			
			Mean	SD	Mean	SD	Mean	SD	Mean	SD
Rain	10	1–2	19.62	2.69	−0.01	0.15	0.11	0.17	26.3	0.8
		2–3	25.88	3.97	−0.03	0.15	0.15	0.16		
		3–4	29.07	6.02	0.00	0.19	0.12	0.17		
		4–5	20.32	6.00	0.08	0.25	0.16	0.22		
		5–6	18.42	11.95	0.45	0.63	0.12	0.17		
Conventional	8	1–2	21.32	1.57	0.06	0.09	0.19	0.22	27.9	1.4
		2–3	33.25	9.42	−0.03	0.06	0.35	0.33		
		3–4	50.98	31.06	0.01	0.03	0.45	0.40		
		4–5	39.49	24.98	−0.08	0.16	0.54	0.50		
		5–6	56.97	55.91	−0.04	0.63	0.60	0.48		

controlling aerosol removal beyond ventilation and deposition. This finding is consistent with previous studies that also observed deviation of total aerosol decay rates from the sum of air exchange rate and deposition rate [12,55]. Additional aerosol removal process may include evaporation, coagulation, diffusional deposition, thermophoresis, inertial impaction as well as interception [29,52,53]. Because the concentrations of micro-sized aerosols measured in the tested scenarios are much less than $10^6/cm^3$, the effect of coagulation on aerosol removal is assumed to be negligible [10]. The diffusional deposition and thermophoresis mainly influence removal of submicron aerosols and have less effect on micro-sized aerosols [23,31,48]. Therefore, evaporation, inertial impaction (particles leave the gas stream and deposit on surfaces) as well as interception (particles follow the gas stream and deposit on surfaces) could be additional removal mechanisms for micro-sized aerosols [53]. These processes can be impacted by the dynamic change of environmental conditions such as temperature and relative

Table 3
Model fitted aerosol generation rates and decay rates under hot water conditions. Note: Aerosol decay rate excludes ventilation rate and deposition rate. SD refers to Standard Deviation, Rain refers to the rain showerhead type, and Conventional refers to the conventional showerhead type.

Showerhead type	Size range (μm)	Aerosol generation rate (μg/min)				Decay rate (1/min)				Water temperature (°C)		Flow rate (L/min)
		Increase state		Steady state		Steady state		Decay stage				
		Mean	SD	Mean	SD	Mean	SD	Mean	SD	Mean	SD	
Rain	1–2	686.8	588.4	257.7	285.7	2.6	2.3	0.8	0.5	40.9	1.1	10
	2–3	4549.4	4130.1	2135.1	2296.1	3.6	4.1	1.4	0.2			
	3–4	23,334.2	24,314.1	9745.4	11,418.2	3.0	3.1	2.6	1.2			
	4–5	61,802.0	66,231.3	17,579.5	17,116.2	2.5	2.5	3.8	2.8			
	5–6	140,471.7	159,349.7	77,192.1	99,972.1	2.1	1.2	5.3	6.3			
	6–7	74,360.3	88,064.7	13,722.9	4906.1	1.2	1.1	5.6	6.6			
	7–8	81,641.0	68,169.5	31,197.7	17,269.3	1.3	0.9	5.4	6.4			
	8–9	100,931.0	71,628.5	52,972.7	30,934.3	1.3	1.1	5.3	6.3			
	9–10	92,473.7	69,256.4	42,300.0	16,300.8	1.2	0.9	5.6	6.7			
Conventional	1–2	614.3	400.8	226.4	290.4	1.0	0.4	1.5	0.4	40.0	0.5	8
	2–3	3482.8	3192.8	934.3	1163.4	0.7	0.2	1.8	0.9			
	3–4	14,702.5	15,197.1	3623.2	5079.4	0.5	0.1	2.3	0.7			
	4–5	31,537.1	39,765.4	7525.8	9056.1	0.5	0.0	2.5	0.7			
	5–6	85,348.3	111,554.5	28,209.1	40,913.1	0.5	0.4	2.3	0.9			
	6–7	89,719.2	109,812.4	18,402.4	16,153.2	0.6	0.2	2.3	1.2			
	7–8	81,574.6	99,626.4	22,565.4	27,268.4	0.4	0.3	2.1	1.1			
	8–9	75,730.2	77,074.2	28,207.7	38,287.5	0.2	0.3	2.0	1.1			
	9–10	79,071.0	85,206.9	21,308.9	25,687.5	0.2	0.2	1.9	1.0			

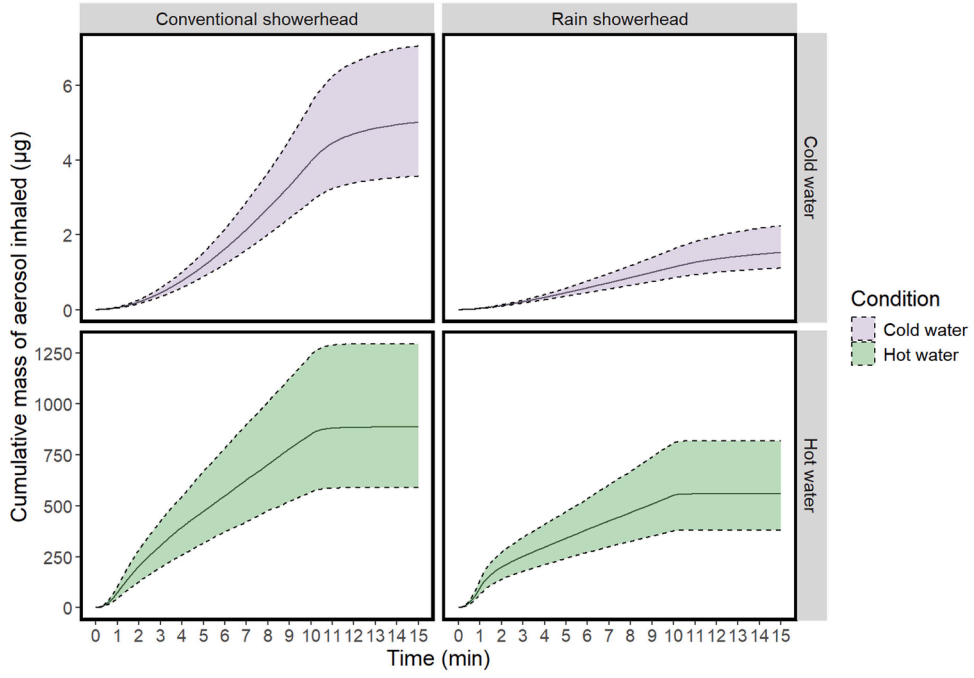

Fig. 4. Estimated mass of aerosols deposited at the alveolar region of an adult over time in cold and hot water conditions for conventional and rain showers. Note: Solid line represents median value and dashed lines represent 5 percentile and 95 percentile values.

humidity and therefore lead to large variations in the fitted aerosol decay rates.

Our model fitted larger aerosol decay rates at the decay stage compared to steady state, suggesting that other process in addition to deposition and ventilation process also play a role on aerosol removal when the shower was turned off. This finding contradicts previous studies which observed no significant difference between aerosol decay rates and the sum of air exchange rate and deposition rate after the shower was turned off [12,52]. A possible explanation for this difference is that air exchange rates and aerosol generation were monitored separately in previous studies. In this study, aerosol concentration and air exchange rate were monitored simultaneously for each shower experiment, allowing higher resolution in the estimate here of the contributions of ventilation rate to aerosol decay processes. Higher aerosol decay rates during the declining stage are reasonable. The lower relative humidity after a shower is turned off can promote evaporation of aerosols, explaining the higher aerosol decay rates during the decay state.

Our modeled aerosol decay rates under hot water conditions were higher than those under cold water conditions, suggesting other processes beyond ventilation and deposition may dominant aerosol removal under hot water conditions. A possible explanation for faster decay of aerosol concentrations under hot water condition than cold water conditions is that thermal plumes can carry micro-sized aerosols upward and lead to direct collisions between aerosols and cold surfaces which is known as the interception [53].

4.3. Implications of dynamic model of aerosol concentration on risk assessment

Our observed initial peak aerosol concentrations under hot water conditions suggest the potential for a high exposure to aerosols within the first few minutes of turning on a shower. Similar instantaneous increases of aerosol concentrations were also observed in previous studies [52,55]. A possible explanation for the instantaneous increase of aerosol concentrations within hot showers is that the thermal plume caused by hot water heating the stall air took concentrated particles to the sampling point [55]. The observed initial increase of carbon dioxide concentrations (Fig. 3A and 3B) also indicated such air movement due to temperature gradients. A potential intervention to reduce exposure to the observed high peak is to avoid entering the shower until aerosol concentrations have stabilized.

Avoiding the first few minutes of aerosol generation may also have impacts on exposures to microorganisms and chemicals. The concentration of waterborne pathogens such as *Legionella* spp. have been observed to be highest in the first draw sample during flushing, likely due to favorable growth conditions (e.g. mixed water temperature, longer stagnation periods as well as elastomeric materials favorable for bacteria growth) in the last meter of pipes connecting to the point of use [9,22,45]. Another factor potentially contributing to the high concentrations of pathogens in the first few liters of shower water is the biofilm detachment process especially for the biofilms developed on old age showerheads [21,40]. The initial biofilm detachment process could lead to fast release of pathogens from the biofilms for the first few minutes during flushing events [28]. Previous studies have directly measured presence of pathogens in air during showers but none of them investigated the temporal dynamics of pathogen concentrations in air [18,36,44]. A combination of factors including an elevated of first draw pathogen concentration with an initial peak concentration of aerosols may result in higher exposures early in the shower period and already lead to a risk above an acceptable threshold. Showering has also been considered as an important exposure route for chemicals present in tap water such as disinfection byproducts as well as heavy metals [7,55]. The concentrations of these chemicals could also be dynamic considering their associations with the presence of microorganisms. For instance, it has been reported that accumulation of heavy metals such as chromium and lead can happen in the biofilms developed in plumbing systems [39]. This suggests that biofilm detachment can also potentially lead to initial high release of heavy metals during flushing. The findings on the initial peak aerosol concentrations within hot showers pose a potential opportunity to develop water and aerosol sampling strategies focusing on first draw concentration for the routine monitoring program.

4.4. Limitations and further improvements for aerosol modelling

The study findings provide a foundation for incorporating dynamic aerosol generation rates in showers into chemical and microbial risk assessments, but several limitations of the data provided also exist. First, isokinetic sampling was not considered during shower experiments. To ensure isokinetic sampling from a gas stream, the free stream velocity should be the same as the gas velocity in the probe. A gas velocity in the probe larger than the free stream velocity will lead to underestimation of particle concentrations while a gas velocity smaller than the free stream velocity will lead to overestimation of particle concentrations. Misalignment which caused by an angle between the sampling probe and gas stream can also lead to underestimation of the particle concentrations [26]. For sampling from still air, the sampling probe should also be placed horizontally instead of vertically to reduce the errors caused by gravity effect [13]. In the evaluated scenarios, the flow of the gas stream was not measured and therefore it is difficult to determine the probe diameter for isokinetic sampling. Second, the dynamics observed are linked to the physical characteristics of the shower studied: other shower stalls with different dimensions, shower head types, flow rates, and ventilation rates may produce different dynamics. Despite this limitation, the modeling approach here provides findings consistent with previous publications as the experimental conditions and shower stall size here are within the previously reported ranges [12,52]. Further, the modeling approach is easily extendable to quantify generation and decay rates from empirical data collected in the future, particularly if the conditions to be modeled are determined to be sufficiently different from the conditions studied here. Second, the study highlights that under some scenarios, incorporation of aerosol removal processes beyond ventilation and deposition may be important for understanding fate and transport of aerosols in showers. The one compartment model investigated decay from sources other than ventilation and deposition by inclusion of an additional residual decay rate. In some scenarios, this residual decay rate was not negligible, suggesting additional aerosol removal processes could be integrated into the mechanistic model. There are several models focusing on aerosol dynamics that also incorporate evaporation and condensation process to account for their evolution of size distribution [15,29,43]. However, such evaporation process should be carefully considered: much larger initial aerosol size means pathogen enrichment might happen due to the shrinkage of aerosols. The relative impact of pathogen enrichment on microbial risk assessment is an area of potential future research including in both laboratory and modeling studies [4,5].

Third, the mass balance model used here is also limited in its generalizability because it does not account for the shifts of aerosol size distribution over time as well as spatial variation of aerosol concentrations within shower stalls. The mass balance model is not able to provide a mechanistic explanation of different aerosol size distributions at cold and hot showers without incorporating the evaporation model for aerosols. However, evaporation models usually focused on the size change of individual aerosol instead of the entire aerosol populations [15,20]. Therefore, incorporating the evaporation model in a population-based mass balance model will be challenging. The results provided here for aerosols sampled at different heights showed that an ideal well-mixed condition was not met due to processes such as a thermal plume, although these results may be biased by the requirement for different tube lengths required for sampling different locations (Figure S7 and S8). Computational fluid dynamics (CFD) modeling approaches are an alternative to one-compartment models that can track the behavior of each individual aerosol. Such aerosol dynamic modelling approaches focus on the behavior of individual aerosols by calculating particle velocity from an initial velocity field, air velocity and external forces such as gravity and friction. Combined with size change of individual aerosols through an evaporation model, the spatial position and size over time of each individual particle can be estimated [15]. Alternatively, the initial particle velocity field can be measured through particle tracking velocimetry (PTV) [18] as parameter input for the aerosol evolution model. In addition, CFD models are more generalizable than mass balance models as they require less scenario-specific data inputs which is a common limitation in applying current risk assessment frameworks. However, validating the CFD model for showers is also challenging as the initial size distributions of droplets generated from showers are difficult to be obtained due to fast evaporation of micro-sized droplets within seconds [51].

5. Conclusions

This study integrated empirical data collection and modeling on aerosol size distributions from showers under multiple scenarios, including hot (39–41 °C) and cold water (25–28 °C) for both conventional and rain showerheads. The resulting data set and fitted model parameters can help to inform microbial and chemical exposure assessments. Notably, the study highlighted that water temperature has a larger influence on aerosol generation rates and aerosol size distributions than showerhead type studied here. Under hot water conditions, large aerosol generation rates occurring in the first minute of a shower

indicate a potential high exposure risk during the first-minute of flushing. Model fitted aerosol decay rates (aerosol removal rates excluding ventilation rate and deposition rate) were higher in hot showers than in cold showers. This finding suggests that removal processes other than ventilation and deposition influence observed concentrations of aerosols in hot showers. The estimated inhalation doses indicated continued exposure to aerosols even after turning off showers at cold water temperatures. The findings suggest that interventions such as reducing hot water temperatures, standing outside of the shower stall for the first 1–2 min after turning on hot showers and exiting the shower stall promptly after turning off cold showers could be effective risk mitigation strategies to reduce aerosol exposures.

Funding

This research was funded by the Federal Food Safety and Veterinary Office (FSVO), in partnership with the Federal Offices of Public Health (FOPH) and Energy (SFOE) in Switzerland, through the project Legionella Control in Buildings (LeCo; Aramis nr.:4.20.01).

CRediT authorship contribution statement

Lizhan Tang: Writing – review & editing, Writing – original draft, Visualization, Validation, Software, Methodology, Investigation, Formal analysis, Data curation, Conceptualization. **Antonia Eichelberg:** Writing – review & editing, Methodology, Investigation. **Franziska Böni:** Writing – review & editing, Methodology, Investigation. **Kerry A. Hamilton:** Writing – review & editing, Methodology, Conceptualization. **Émile Sylvestre:** Writing – review & editing, Methodology, Conceptualization. **Frederik Hammes:** Writing – review & editing, Resources, Project administration, Methodology, Funding acquisition, Conceptualization. **Timothy R Julian:** Writing – review & editing, Supervision, Resources, Project administration, Methodology, Funding acquisition, Conceptualization.

Declaration of competing interest

The authors declare the following financial interests/personal relationships which may be considered as potential competing interests:

Timothy R. Julian reports financial support was provided by Swiss Federal Food Safety and Veterinary Office. If there are other authors, they declare that they have no known competing financial interests or personal relationships that could have appeared to influence the work reported in this paper.

Acknowledgements

We thank Jing Wang for aid in the experimental design and analysis.

Supplementary materials

Supplementary material associated with this article can be found, in the online version, at doi:10.1016/j.buildenv.2025.112825.

Data availability

Data are available at: https://doi.org/10.25678/000DPZ.

References

[1] M. Al-Shammiri, Evaporation rate as a function of water salinity, Desalination 150 (2) (2002) 189–203.
[2] S. Allegra, L. Leclerc, P.A. Massard, F. Girardot, S. Riffard, J. Pourchez, Characterization of aerosols containing Legionella generated upon nebulization, Sci. Rep. 6 (1) (2016) 33998.
[3] S. Allegra, S. Riffard, L. Leclerc, F. Girardot, M. Stauffert, V. Forest, J. Pourchez, A valuable experimental setup to model exposure to Legionella's aerosols generated by shower-like systems, Water Res. 172 (2020) 115496.
[4] T.W. Armstrong, C.N. Haas, Legionnaires' disease: evaluation of a quantitative microbial risk assessment model, J. Water. Health 6 (2) (2008) 149–166.
[5] T.W. Armstrong, C.N. Haas, Quantitative microbial risk assessment model for Legionnaires' disease: assessment of human exposures for selected spa outbreaks, J. Occup. Environ. Hyg. 4 (8) (2007) 634–646.
[6] C.G. Association, Carbon dioxide. in: Handbook of Compressed Gases, Springer, 1978, pp. 295–311.
[7] L.C. Backer, D.L. Ashley, M.A. Bonin, F.L. Cardinali, S.M. Kieszak, J.V. Wooten, Household exposures to drinking water disinfection by-products: whole blood trihalomethane levels, J. Expo Sci. Environ. Epidemiol. 10 (4) (2000) 321–326.
[8] S. Batterman, Review and extension of CO2-based methods to determine ventilation rates with application to school classrooms, Int. J. Environ. Res. Public Health 14 (2) (2017) 145.
[9] E. Bédard, K. Paranjape, C. Lalancette, M. Villion, C. Quach, C. Laferrière, S. P. Faucher, M. Prévost, Legionella pneumophila levels and sequence-type distribution in hospital hot water samples from faucets to connecting pipes, Water Res. 156 (2019) 277–286.
[10] R. Cai, E. Häkkinen, C. Yan, J. Jiang, M. Kulmala, J. Kangasluoma, The effectiveness of the coagulation sink of 3–10 nm atmospheric particles, Atmos. Chem. Phys. 22 (17) (2022) 11529–11541.
[11] S. Chattopadhyay, S.D. Perkins, M. Shaw, T.L. Nichols, Evaluation of exposure to Brevundimonas diminuta and Pseudomonas aeruginosa during showering, J. Aerosol. Sci. 114 (2017) 77–93.
[12] K.A. Cowen, W.M. Ollison, Continuous monitoring of particle emissions during showering, J. Air Waste Manage. Assoc. 56 (12) (2006) 1662–1668.
[13] C. Davies, The entry of aerosols into sampling tubes and heads, J. Phys. D. Appl. Phys. 1 (7) (1968) 921.
[14] K. Dean, J. Mitchell, Reverse QMRA for Pseudomonas aeruginosa in premise plumbing to inform risk management, J. Environ. Eng. 146 (3) (2020) 04019120.
[15] S. Dhawan, P. Biswas, Aerosol dynamics model for estimating the risk from short-range airborne transmission and inhalation of expiratory droplets of SARS-CoV-2, Environ. Sci. Technol. 55 (13) (2021) 8987–8999.
[16] S. Dhawan, P. Biswas, Sampling artifacts in denuders during phase partitioning measurements of semi-volatile organic compounds, Aerosol Sci. Technol. 53 (1) (2019) 73–85.
[17] U.S. Epa, Exposure Factors Handbook, 20460, Office of research and Development, Washington, DC, 2011, pp. 2–6.
[18] C. Estrada-Perez, K. Kinney, J. Maestre, Y. Hassan, M. King, Droplet distribution and airborne bacteria in an experimental shower unit, Water Res. 130 (2018) 47–57.
[19] J.O. Falkinham III, Living with Legionella and other waterborne pathogens, Microorganisms 8 (12) (2020) 2026.
[20] J.-N. Fan, M. Qiao, Y. Yang, Y. Wang, C. Huan, Y. Huang, Y. Cao, Mathematical modeling of multi-component aerosol droplet evaporation and growth in indoor environments, J. Hazard. Mater. (2024) 134837.
[21] L.M. Feazel, L.K. Baumgartner, K.L. Peterson, D.N. Frank, J.K. Harris, N.R. Pace, Opportunistic pathogens enriched in showerhead biofilms, Proc. Natl. Acad. Sci. 106 (38) (2009) 16393–16399.
[22] M. Grimard-Conea, E. Deshommes, E. Doré, M. Prévost, Impact of recommissioning flushing on Legionella pneumophila in a large building during the COVID-19 pandemic, Front. Water 4 (2022) 959689.
[23] A. Guha, Transport and deposition of particles in turbulent and laminar flow, Annu Rev. Fluid. Mech. 40 (1) (2008) 311–341.
[24] K.A. Hamilton, W. Ahmed, S. Toze, C.N. Haas, Human health risks for Legionella and Mycobacterium avium complex (MAC) from potable and non-potable uses of roof-harvested rainwater, Water Res. 119 (2017) 288–303.
[25] K.A. Hamilton, M.T. Hamilton, W. Johnson, P. Jjemba, Z. Bukhari, M. Lechevallier, C.N. Haas, P.L. Gurian, Risk-Based critical concentrations of legionella pneumophila for indoor residential water uses, Environ. Sci. Technol. 53 (8) (2019) 4528–4541.
[26] W.C. Hinds, Y. Zhu, Aerosol technology: properties, behavior, and Measurement of Airborne Particles, John Wiley & Sons, 2022.
[27] S.A. Hines, D.J. Chappie, R.A. Lordo, B.D. Miller, R.J. Janke, H.A. Lindquist, K. R. Fox, H.S. Ernst, S.C. Taft, Assessment of relative potential for Legionella species or surrogates inhalation exposure from common water uses, Water Res. 56 (2014) 203–213.
[28] C. Huang, Y. Shen, R.L. Smith, S. Dong, T.H. Nguyen, Effect of disinfectant residuals on infection risks from Legionella pneumophila released by biofilms grown under simulated premise plumbing conditions, Environ. Int. 137 (2020) 105561.
[29] T. Hussein, H. Korhonen, E. Herrmann, K. Hämeri, K.E. Lehtinen, M. Kulmala, Emission rates due to indoor activities: indoor aerosol model development, evaluation, and applications, Aerosol Sci. Technol. 39 (11) (2005) 1111–1127.
[30] N. Ibáñez-Rueda, J. Guardiola, S. López-Ruiz, F. González-Gómez, Towards a sustainable use of shower water: habits and explanatory factors in southern Spain, Sustain. Water Resour. Manage. 9 (4) (2023) 121.
[31] H. Kim, C. Jung, S. Oh, K. Lee, Particle removal efficiency of gravitational wet scrubber considering diffusion, interception, and impaction, Environ. Eng. Sci. 18 (2) (2001) 125–136.
[32] A.C. Lai, W.W. Nazaroff, Modeling indoor particle deposition from turbulent flow onto smooth surfaces, J. Aerosol. Sci. 31 (4) (2000) 463–476.
[33] E.R. Lewis, The effect of surface tension (Kelvin effect) on the equilibrium radius of a hygroscopic aqueous aerosol particle, J. Aerosol. Sci. 37 (11) (2006) 1605–1617.

[34] F. Marcoline, M. Grabe, S. Nayak, T. Zahnley, G. Oster, R. Macey, Berkeley Madonna User's Guide, Berkeley Madonna, Inc., Albany, CA, 2020.
[35] H. Niculita-Hirzel, S. Goekce, C.E. Jackson, G. Suarez, L. Amgwerd, Risk exposure during showering and water-saving showers, Water 13 (19) (2021) 2678.
[36] H. Niculita-Hirzel, M. Morales, P. Parmar, Assessing the health risks associated with the usage of water-atomization shower systems in buildings, Water Res. 243 (2023) 120413.
[37] H. Niculita-Hirzel, A.S. Vanhove, L. Leclerc, F. Girardot, J. Pourchez, S. Allegra, Risk exposure to Legionella pneumophila during showering: the difference between a classical and a water saving shower system, Int. J. Environ. Res. Public Health 19 (6) (2022) 3285.
[38] J. O'Toole, M. Keywood, M. Sinclair, K. Leder, Risk in the mist? Deriving data to quantify microbial health risks associated with aerosol generation by water-efficient devices during typical domestic water-using activities, Water Sci. Technol. 60 (11) (2009) 2913–2920.
[39] P. Parmar, H. Niculita-Hirzel, The accumulation of heavy metals in shower system biofilms: implications for emissions and indoor human exposure, Pollutants 3 (3) (2023) 396–405.
[40] S. Pitell, S.-J. Haig, Assessing the impact of anti-microbial showerheads on the prevalence and abundance of opportunistic pathogens in shower water and shower water-associated aerosols, Front. Microbiomes 2 (2023) 1292571.
[41] S. Pitell, C. Woo, E. Trump, S.-J. Haig, Balancing water conservation and health: do water-saving showerheads impact the microbes we breathe in during showering? Front. Microbiomes 3 (2024) 1416055.
[42] H. Sales-Ortells, G. Medema, Screening-Level microbial risk assessment of urban water locations: a tool for prioritization, Environ. Sci. Technol. 48 (16) (2014) 9780–9789.
[43] C. Seigneur, A.B. Hudischewskyj, J.H. Seinfeld, K.T. Whitby, E.R. Whitby, J. R. Brock, H.M. Barnes, Simulation of aerosol dynamics: a comparative review of mathematical models, Aerosol Sci. Technol. 5 (2) (1986) 205–222.
[44] Y. Shen, S.-J. Haig, A.J. Prussin, J.J. LiPuma, L.C. Marr, L. Raskin, Shower water contributes viable nontuberculous mycobacteria to indoor air, PNAS Nexus 1 (5) (2022) pgac145.
[45] Y. Shen, C. Huang, J. Lin, W. Wu, N.J. Ashbolt, W.-T. Liu, T.H. Nguyen, Effect of disinfectant exposure on Legionella pneumophila associated with simulated drinking water biofilms: release, inactivation, and infectivity, Environ. Sci. Technol. 51 (4) (2017) 2087–2095.
[46] K. Simpson, C. Staddon, S. Ward, Challenges of researching showering routines: from the individual to the socio-material, Urban Sci. 3 (1) (2019) 19.
[47] H. Smith, Human respiratory tract model for radiological protection, ICRP Publication 66 (1994).
[48] P. Tandon, J.P. Terrell, X. Fu, A. Rovelstad, Estimation of particle volume fraction, mass fraction and number density in thermophoretic deposition systems, Int. J. Heat. Mass Transf. 46 (17) (2003) 3201–3209.
[49] L. Tang, W.J. Rhoads, A. Eichelberg, K.A. Hamilton, T.R. Julian, Applications of quantitative microbial risk assessment to respiratory pathogens and implications for uptake in policy: a state-of-the-science review, Environ. Health Perspect. 132 (5) (2024) 056001.
[50] R. Tang, Y. Etzion, Comparative studies on the water evaporation rate from a wetted surface and that from a free water surface, Build. Environ. 39 (1) (2004) 77–86.
[51] X. Xie, Y. Li, A. Chwang, P. Ho, W. Seto, How far droplets can move in indoor environments–revisiting the wells evaporation–falling curve, Indoor Air 17 (3) (2007).
[52] X. Xu, C.P. Weisel, Inhalation exposure to haloacetic acids and haloketones during showering, Environ. Sci. Technol. 37 (3) (2003) 569–576.
[53] X. Zhang, Z. Gan, Y. Li, Collection of particles on cold surfaces: a review, Ind. Eng. Chem. Res. 59 (38) (2020) 16493–16506.
[54] X. Zhang, Z. Ji, Y. Yue, H. Liu, J. Wang, Infection risk assessment of COVID-19 through aerosol transmission: a case study of South China seafood market, Environ. Sci. Technol. 55 (7) (2020) 4123–4133.
[55] Y. Zhou, J.M. Benson, C. Irvin, H. Irshad, Y.-S. Cheng, Particle size distribution and inhalation dose of shower water under selected operating conditions, Inhal. Toxicol. 19 (4) (2007) 333–342.
[56] Y. Zhou, K.W. Mui, L.T. Wong, P.H. Tsui, W.K. Chan, Aerosol generation rates for showerheads, Build. Services Eng. Res. Technol. 40 (5) (2019) 595–610.